IEEE Access
Multidisciplinary | Rapid Review | Open Access Journal

Received 13 January 2023, accepted 26 January 2023, date of publication 27 February 2023, date of current version 2 March 2023.

Digital Object Identifier 10.1109/ACCESS.2023.3249819

RESEARCH ARTICLE

Design of the Wideband and Low-Height Omnidirectional Cylindrical Dielectric Resonator Antenna Using Arced-Apertures Feeding

XIAO SHENG FANG[1,2,3], (Member, IEEE), LING PENG WENG[1,3], (Student Member, IEEE), AND ZHUN FAN[1,3], (Senior Member, IEEE)

[1]Department of Electronic and Information Engineering, Shantou University, Shantou 515063, China
[2]The State Key Laboratory of Millimeter Waves, Southeast University, Nanjing 211189, China
[3]Guangdong Provincial Key Laboratory of Digital Signal and Image Processing, Shantou University, Shantou 515063, China

Corresponding author: Xiao Sheng Fang (fangxs@stu.edu.cn)

This work was supported in part by the Guangdong Basic and Applied Basic Foundation under Grant 2022A1515010248, in part by the Department of Education of Guangdong Province under Grant 2020ZDZX3015, and in part by the Open Project of State Key Laboratory of Millimeter Waves under Grant K202237.

ABSTRACT This paper mainly discusses the design of wideband and low-height omnidirectional cylindrical dielectric resonator antenna (DRA). It was theoretically found that the TM-mode category of the cylindrical DRA is suitable for the wideband and low-height design using mode-merging method ($TM_{01\delta}$ and $TM_{02\delta}$ mode). An improved apertures-fed technique is proposed to excite the TM-mode DRA. The feeding consists of four arc-shaped apertures, and each aperture was fed by the in-phase signal. Based on the E-field distribution, the higher-order $TM_{02\delta}$ mode of the cylindrical DRA can be excited by adjusting the position of the apertures, and it fuses together with the fundamental $TM_{01\delta}$ mode to achieve a wideband antenna. Besides, the aperture mode further widen its impedance bandwidth. To demonstrate the idea, a wideband and low-height omnidirectional cylindrical glass DRA was designed for WLAN 5.2-GHz and 5.8-GHz applications. The experimental results show that the proposed low-height DRA ($h = 0.108\lambda_0$) can achieve an impedance bandwidth of 25.2 % (without aperture mode) and 34 % (with aperture mode), respectively. The bandwidth enhancement of the proposed design is significant, compared to other reported low-height TM-mode DRAs.

INDEX TERMS Cylindrical DRA, TM-mode, low-height, wideband.

I. INTRODUCTION

For indoor communication, omnidirectional antenna has gained in popularity because it is able to provide a relatively wide coverage. In the past three decades, a large number of studies have shown that the dielectric resonator antenna (DRA) [1], [2], [3], [4], [5] owns the merits of low loss, high radiation efficiency and controllable bandwidth. In addition, the electric dipole mode (TM-mode) of the DRA providing the omnidirectional radiation pattern is very easy to be excited [6], [7], [8], [9], making it a good candidate for designing the omnidirectional antenna.

The associate editor coordinating the review of this manuscript and approving it for publication was Tutku Karacolak.

Nowadays, there are various types of portable electronic devices for wireless communication application, and these devices are usually very small in thickness. Hence, antennas with low-height feature are urgently required [10], [11], [12], [13]. For example, in [11], an omnidirectional DRA with a height of h = $0.08\lambda_0$ was excited by a probe, but it only has an impedance bandwidth of $\sim$ 3 %. Some effort has been paid on the design of the wideband and low-height omnidirectional DRAs [12], [13]. For instance, by using the metal-via technique, the higher-order mode of the low-height DRA (h = $0.09\lambda_0$) can be excited and merged with the fundamental mode to achieve an impedance bandwidth of $\sim$ 9 % [12]. By increasing the radius of the probe in the DRA, the impedance bandwidth of the low-height DRA

($h = 0.11\lambda_0$) can be increased to $\sim$ 17 % [13], but the cost is that a large air region is required to dig. In general, the impedance bandwidth of a low-height omnidirectional DRA is relatively limited when the probe-fed method is employed.

The DRA can be fed by using many planar-fed techniques such as microstrip line [14], [15], aperture [16], [17] and coplanar waveguide [18], [19], but they are mainly applied to design the broadside DRA. Recently, several planar-fed methods have been proposed to excite the omnidirectional DRA, which can be divided into two kinds. The first one is to use the TE-mode DRA [20], [21]. For this method, two DRA elements are always needed, and one of the DRA elements is required to be inserted into the substrate, making the fabrication relatively complex. The second method is to employ the TM-mode DRA. For example, in [22], a microstrip end-shorted cross patch forming an equivalent vertical electric monopole is adopted to excite the $TM_{01\delta}$-mode of the cylindrical DRA. Its disadvantage is that shorting pins are needed for the design. In [23], the $TM_{01\delta}$-mode of the cylindrical DRA is excited by an annular aperture. This is a pin-free method, but it requires mender lines to optimize the DRA. In [24], the author uses four inclined apertures to excite a circularly polarized omnidirectional DRA. In this way, no shorting pins or meander lines are required.

In this paper, design of the wideband and low-height TM-mode cylindrical DRA is discussed. The proposed low-height TM-mode DRA is excited by an improved aperture-fed method, which consists of four arced apertures perpendicular to the radial direction. Observing the E-field distribution, the higher-order $TM_{02\delta}$ modes of the cylindrical DRA can be excited by adjusting the position of the aperture, and it merges with the $TM_{01\delta}$ mode to form a wideband antenna. The feasibility of this idea is proved theoretically and practically. Also, the effect of the apertures on the performance of the DRA is discussed in detail. ANSYS HFSS was employed to simulate the proposed DRA and experiment was carried out to verify it. The antenna performance, including the VSWR, radiation pattern and antenna gain were studied. It turns out that the proposed low-height DRA ($h = 0.108\lambda_0$) provides an impedance bandwidth of $\sim$ 34 %, completely covering WLAN 5.2-GHz and 5.8-GHz bands.

II. THEORY, EXCITATION, AND ANTENNA CONFIGURATION

A. FEASIBILITY

Figure 1 shows a cylindrical DRA locating on a circular ground plane, which has a permittivity of ε_r, a radius of a and a height of h. In this paper, the $TM_{01\delta}$ and $TM_{02\delta}$ modes of the cylindrical DRA are employed. Its feasibility is proved theoretically in this part. Figure 2 shows the frequency ratio $f_{(TM02\delta)}$ / $f_{(TM01\delta)}$ changes with h/a, which is calculated by using the formula (A1) in the Appendix. To achieve a wideband DRA, $f_{(TM02\delta)}$ / $f_{(TM01\delta)}$ are required to be small enough so that the two modes can be merged together. Referring to the figure, decreasing $f_{(TM02\delta)}$ / $f_{(TM01\delta)}$ would decrease h. with the radius a kept unchanged. This result shows it

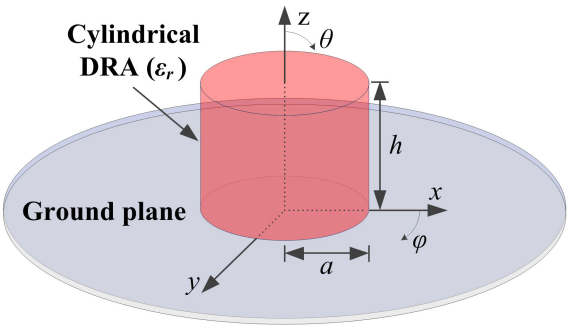

FIGURE 1. Cylindrical DRA locating on a circular ground plane.

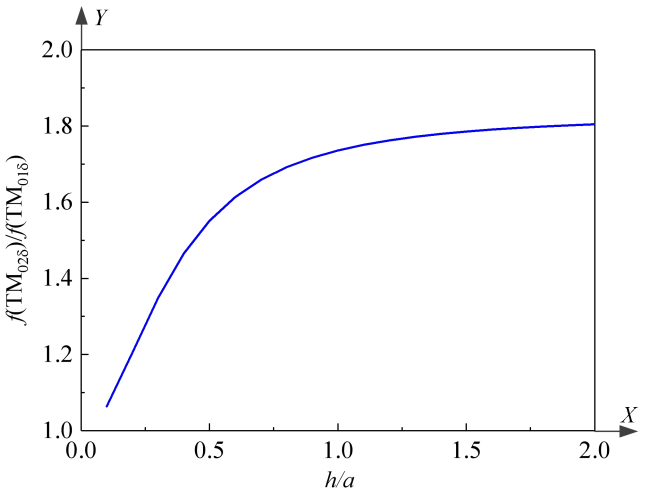

FIGURE 2. Resonant frequency ratio $f_{(TM02\delta)}$ / $f_{(TM01\delta)}$ as a function of h/a ($\varepsilon_r = 10$).

is possible to use the mode-merging method to achieve a wideband cylindrical DRA when its height is low.

B. EXCITATION

In this paper, arced apertures are proposed to feed the TM-mode DRA. Figure 3 shows the simplified structure of the proposed cylindrical DRA fed by different number of the arced apertures. The cylindrical DRA has a permittivity of $\varepsilon_r = 6.85$ (K9-glass), a radius of $a = 25$ mm and a height of $h = 5.5$ mm ($0.108\lambda_0$). Using the formula (A1) in Appendix I, the estimated resonance frequency of the $TM_{01\delta}$ mode is calculated as 5.91 GHz. In the design, each arced aperture equivalent to a magnetic current unit were placed perpendicular to the radial direction. They were fed by a 50 Ω microstrip line terminated by the in-phase excitation port with the same input power amplitude. In this way, the H-field of the apertures form a circular shape on the horizontal plane, which can be equivalent to a vertical electric dipole. The effect of the aperture number on the performance of the DRA is investigated in Figure 3, with the aperture number N equal to 2, 4 and 8. For a fair comparison, the aperture lengths of the three cases are set as $L_1 = 2L_2 = 4L_3$ ($L_3 = 6.8$ mm). The corresponding simulated H-plane radiation patterns of the $TM_{01\delta}$ mode of the DRA at 5.91 GHz are presented in Figure 4.

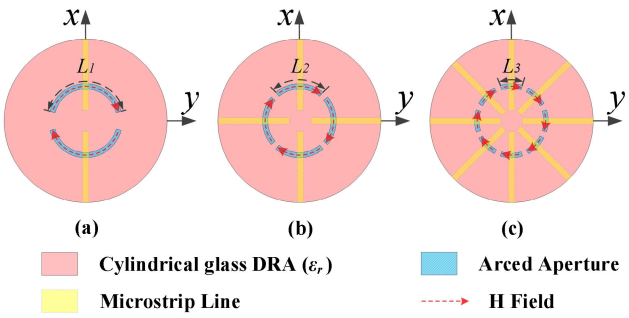

FIGURE 3. Cylindrical DRA fed by different number of the apertures ($L_1 = 2L_2 = 4L_3$). (a) Two apertures. (b) Four apertures. (c) Eight apertures.

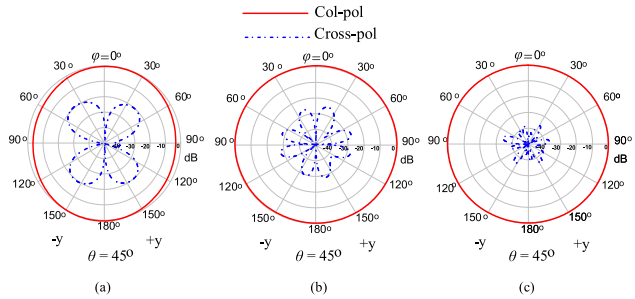

FIGURE 4. Simulated radiation pattern at H-plane of the $TM_{01\delta}$ mode of the cylindrical DRA shown in Figure 3. (a) Two apertures. (b) Four apertures. (c) Eight apertures.

Referring to the figure, the DRA shows omnidirectional characteristics for the three cases, as expected. When $N = 2$, the col-pol fields at $\Phi = \pm 90^{\circ}$ are relatively weak, resulting in a bad omnidirectivity for the DRA. As the number of the apertures increases, the omnidirectivity of the DRA becomes better. Good omnidirectional radiation can be obtained when $N \geq 4$ (eg. $N = 4, 8$). However, more apertures mean more complex feeding network. Therefore, $N = 4$ is chosen in our design. It should be mentioned that the length of apertures would not obviously affect the omnidirectivity of the DRA.

Next, the shape of the aperture on the radiation performance of the antenna is discussed. Figure 5 presents the simplified configuration of the proposed cylindrical DRA fed by the rectangular, U-shaped and arc-shaped apertures, respectively. Their corresponding simulated antenna gain in the azimuth plane are given in Figure 6. As can be found from the figure, the gain fluctuations (|max.|-|min.|) for the rectangular, U-shaped and arc-shaped apertures are 1.44, 1.29 and 1.18 dB, respectively, showing using arc-shaped aperture can have the best omnidirectivity. This is expected since the arced aperture is mostly closed to the shape of the omnidirectional radiation pattern. Based on the above analysis, arced apertures with $N = 4$ are chosen in our final design.

C. ANTENNA CONFIGURATION

Figure 7 shows the final configuration of the proposed apertures-fed low-height TM-mode cylindrical DRA. Four

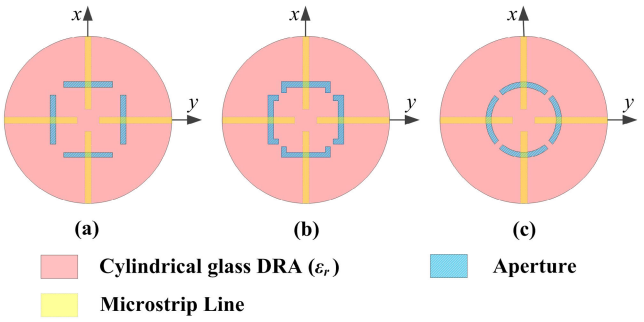

FIGURE 5. Cylindrical DRA fed by the apertures with different shapes. (a) Rectangular. (b) U-shaped. (c) Arc-shaped.

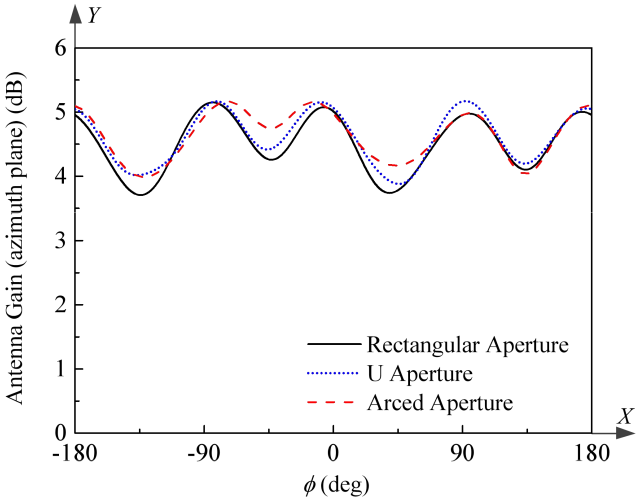

FIGURE 6. Simulated antenna gains in the azimuth plane of the cylindrical DRA fed by different aperture shapes: rectangular, U-shaped and arc-shaped.

arced apertures were printed on the top face of a circular substrate, which has a permittivity of $\varepsilon_{rs} = 2.94$, a height of $h_s = 0.762$ mm and a diameter of $d_g = 130$ mm. Each arced aperture has a length of $L = 13.6$ mm and a width of $W = 1.6$ mm, with a distance of d=10.5 mm from the middle of the DRA. A power divider for providing the 4-way in-phase signals was printed at the bottom face of the substrate, with its center frequency designed at ~5.8 GHz. It should be mentioned that the power divider here can improve the impedance matching of the DRA, which can be regarded as a matching network. 50-Ω microstrip feedline ($W_f = 1.94$ mm) was employed to supply the power for the apertures, with a stub length of $L_s = 7.2$ mm and a stub width of $W_s = 0.97$ mm for the matching.

D. MODE ANALYSIS

Mode analysis is carried out in this section. The effect of the aperture position d on the performance of the DRA is investigated first. Figure 8 presents the simulated VSWRs of the proposed DRA for different d. Referring to the figure, the DRA is not well excited when d is relatively small (eg. $d = 5$mm). As d increases, the matching of the $TM_{01\delta}$

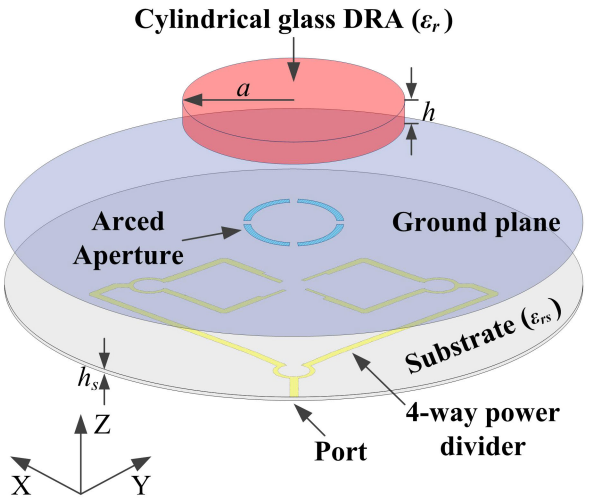

(a)

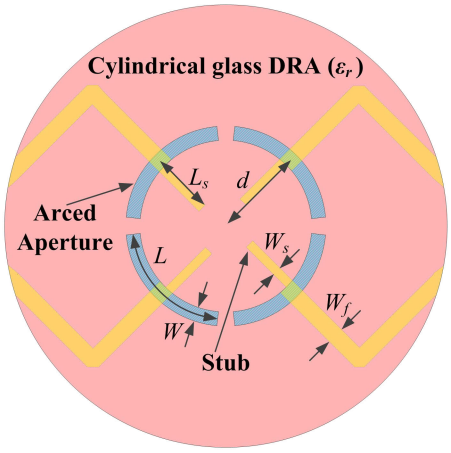

(b)

FIGURE 7. The configuration of the apertures-fed low-height and wideband cylindrical DRA: $\varepsilon_r = 6.85$, $a = 25$ mm, $h = 5.5$ mm, $L = 13.6$ mm, $W = 1.6$ mm, $\varepsilon_{rs} = 2.94$, $h_s = 0.762$ mm, $W_f = 1.94$ mm, $d = 10.5$ mm, $L_s = 7.2$ mm and $W_s = 0.97$ mm. (a) 3D view. (b) Top view of the cylindrical DRA and apertures.

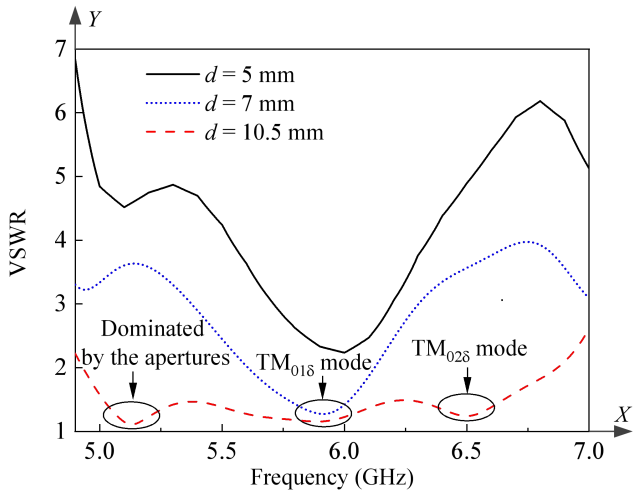

FIGURE 8. Simulated VSWRs of the proposed apertures-fed low-height and wideband cylindrical DRA vs frequency for different d. Other parameters are the same as in Figure 7.

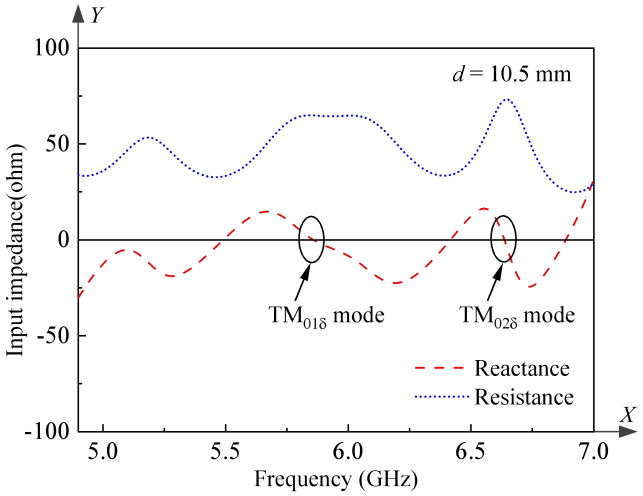

FIGURE 9. Simulated input impedance of the proposed DRA vs frequency as $d = 10.5$ mm. Other parameters are the same as in Figure 7.

mode becomes better. Figure 9 shows the simulated input impedance of the proposed DRA when $d = 10.5$ mm. Referring to the figure, the $TM_{01\delta}$ and $TM_{02\delta}$ modes of the cylindrical DRA are simultaneously excited at 5.86 GHz and 6.64 GHz, respectively, with their estimated resonance frequencies calculated using the formula (A1) (Appendix) as 5.91 GHz (0.8 % error) and 6.91 GHz (3.9 % error). The error of the simulated $TM_{02\delta}$-mode resonance frequency is relatively large, which is due to the loading effect. From the result of VSWR in Figure 8, one more resonant mode at 5.2 GHz is observed, which is dominated by the apertures, with the estimated resonance frequency of each aperture equal to 5.0 GHz (3.8 % error) using $f_s = 0.5c/(L\sqrt{(\varepsilon_{rs} + \varepsilon_r)/2})$.

The E-fields of the $TM_{01\delta}$ and $TM_{02\delta}$ modes of the cylindrical DRA ($d = 10.5$ mm) are given in Figure 10. With reference to the figure, typical E fields of the $TM_{01\delta}$ and $TM_{02\delta}$ modes are observed. Besides, it can be seen from Figure 10 (b) that the E field of the $TM_{02\delta}$ mode is very strong around $x = \pm 0.5a$, indicating the position of the aperture should be closed to $0.5a$ for successfully exciting the $TM_{02\delta}$ mode. This explains why d =10.5 mm can have a good matching for the $TM_{02\delta}$ mode in Figure 8. In addition, the field at 5.2 GHz formed by the four apertures is similar to the $TM_{01\delta}$ mode, which is important because it ensure the consistency of radiation pattern in the whole frequency band.

To further verify the resonance modes, the effect of the DRA dimension on its performance is studied. Figure 11 shows the simulated VSWRs for different height h. As can be seen from the figure, increasing h would shift the second and third resonance modes to the left but have little effect on the frequency of the first resonance mode, showing the first resonance mode is due to the apertures and the other two

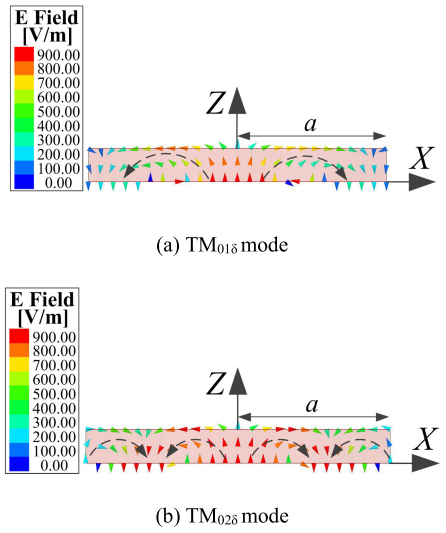

FIGURE 10. Simulated E-field in elevation (x–z) plane for the proposed apertures-fed low-height cylindrical DRA. The parameters are the same as in Figure 7. (a) 5.86 GHz. (b) 6.64 GHz.

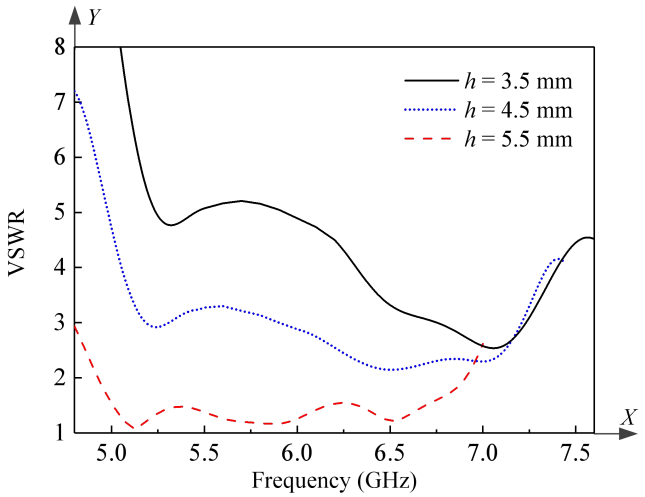

FIGURE 11. Simulated VSWRs of the proposed apertures-fed low-height cylindrical DRA vs frequency for different h. Other parameters are the same as in Figure 7.

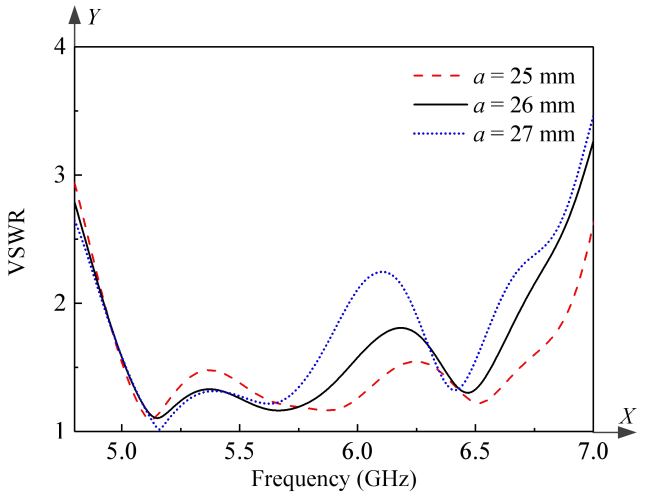

FIGURE 12. Simulated VSWRs of the proposed apertures-fed low-height cylindrical DRA vs frequency for different a. Other parameters are the same as in Figure 7.

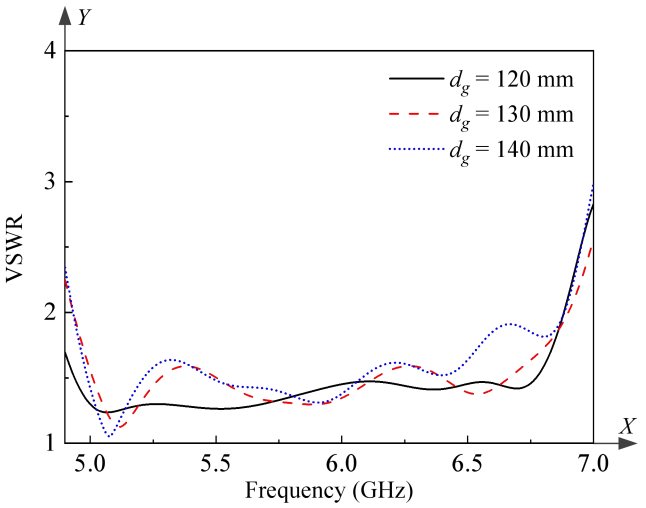

FIGURE 13. Simulated VSWRs of the proposed apertures-fed low-height cylindrical DRA vs frequency for different diameters of the ground plane. Other parameters are the same as in Figure 7.

modes are due to the DRA. Additionally, increasing h would improve the matching of the DRA, and thus enlarging its impedance bandwidth. An optimal impedance bandwidth can be achieved when $h = 5.5$ mm. Figure 12 shows the simulated VSWRs for different radius a. Similarly, increasing a would move the second and third resonance modes to the left but do not affect the first resonance mode too much. Besides, it is observed that a can be used to tune the matching between two DRA modes. The effect of the aperture length and width on the performance of the DRA was also studied. It was found that these two parameters do not affect the matching and bandwidth of the DRA too much. For brevity, the result is not shown here. Besides, the effect of the size of the ground plane on the reflection coefficient of the proposed antenna is studied in Figure 13. It is found that changing the diameter of the ground plane has relatively small effect on the reflection coefficient.

III. EXPERIMENTAL RESULT

Based on the previous results, a wideband and low-height cylindrical DRA was fabricated by using K9 glass, with its prototype shown in Figure 14. Referring to the figure, the DRA has a thin and transparent appearance. Figure 15 displays the VSWRs of the DRA. With reference to the figure, the measured impedance bandwidth (VSWR $\leq$ 2) of the proposed DRA without considering aperture mode is 25.2 % (5.34–6.88 GHz), while the impedance bandwidth of the proposed DRA is obtained as 34 % (4.88–6.88 GHz) when taking the aperture mode into account.

Figure 16 (a) and (b) display the radiation patterns of the $TM_{01\delta}$ and $TM_{02\delta}$ modes of the DRA, respectively. The

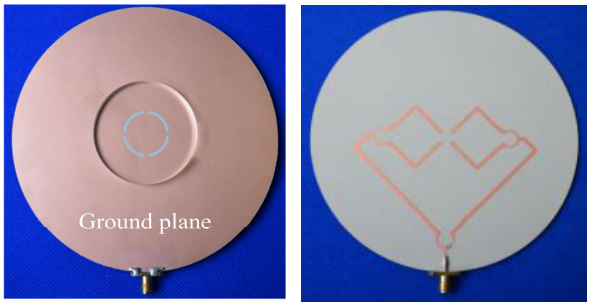

FIGURE 14. The prototype of the apertures-fed wideband and low-height cylindrical DRA. (a) Top view. (b) Bottom view. The parameters are the same as in Figure 7.

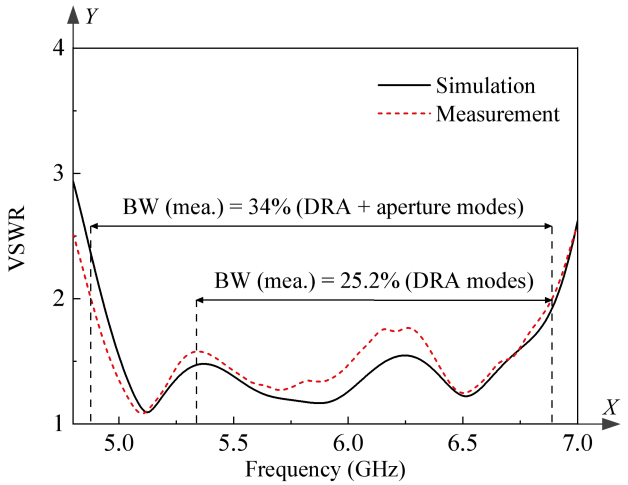

FIGURE 15. Measured and simulated VSWRs of the proposed apertures-fed wideband and low-height cylindrical DRA vs frequency.

TABLE 1. Comparison of the different low-height tm-mode DRAS.

Reference	ε_r	Height (H/λ_0)	BW (%)	Peak gain (dBi)	Mode
[10]	9.2	~0.05	1.7	~	$TM_{01\delta}$
[11]	20	~0.08	2.5	~	$TM_{01\delta}$
[12]	~	~0.09	8.9	1.8	$TM_{01\delta}$, $TM_{02\delta}$
[13]	38	~0.11	17	0.8	$TM_{01\delta}$
Pro. (without considering aperture mode)	6.85	0.108	25.2	5.16	$TM_{01\delta}$, $TM_{02\delta}$
Pro.(with considering aperture mode)	6.85	0.108	34	5.16	$TM_{01\delta}$,$TM_{02\delta}$, apertures

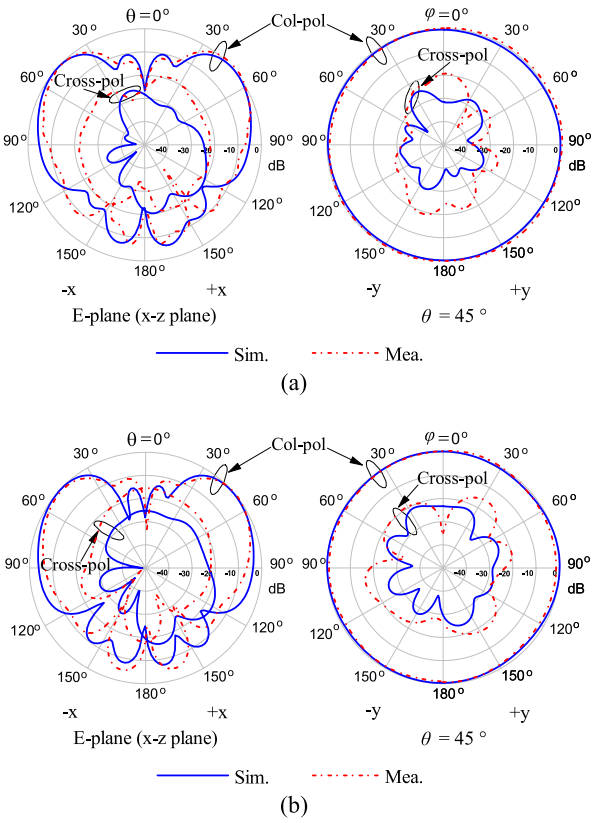

FIGURE 16. Measured and simulated radiation patterns of the proposed apertures-fed low-height cylindrical DRA. (a) 5.8 GHz. (b) 6.5 GHz.

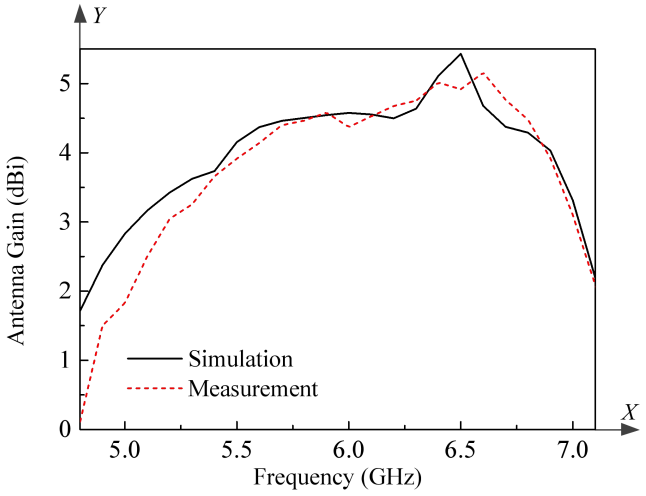

FIGURE 17. Measured and simulated antenna gains of the proposed apertures-fed low-height cylindrical DRA vs frequency.

measured and simulated results are in reasonable agreement. Symmetrical radiation patterns were obtained at E-plane for both resonant modes. It is worth mentioning that the maximum radiation field has a 45° tilting angle because a large ground plane ($d_g = 2.55\lambda_0$) is employed. Additionally, good omnidirectional radiation patterns were observed at the azimuth plane of $\theta = 45°$. Figure 17 displays the antenna gain ($\theta = 45°$ and $\varphi = 0°$) of the DRA. A relatively large peak gain was measured as 5.16 dBi at 6.6 GHz, which is due to the use of high-order $TM_{02\delta}$ mode. Additionally, a large ground plane used in the design will also improve the gain level overall. Undeniably, the large ground plane would increase the transverse dimension, which is the cost of the proposed design. The measured efficiency of the proposed DRA is

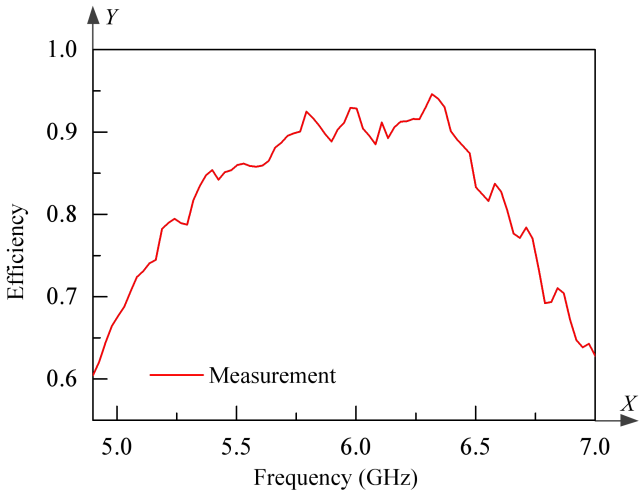

FIGURE 18. Measured antenna efficiency of the proposed apertures-fed low-height cylindrical DRA vs frequency.

shown in Figure 18. Its range is from 0.6 to 0.94 over the target band.

The impedance bandwidth of the proposed low-height DRA is evaluated here. Table 1 compares our DRA with other reported low-height ($h \leq 0.11\lambda_0$) TM-mode cylindrical DRAs. As can be seen from the table, the height of the DRA (0.052 λ_0) in [10] is smallest, but its impedance bandwidth (1.7 %) is narrowest. Increasing the height can enlarge the impedance bandwidth, which has been verified in [11], [12], [13], and [14]. For our case, the height of the DRA is about two times larger than that in [10]. But the impedance bandwidths of the DRA without and with considering the aperture mode are about 14 and 20 times wider than that in [10], respectively, which shows the bandwidth enhancement of our design is significant.

IV. CONCLUSION

In this paper, an apertures-fed wideband and low-height cylindrical DRA has been investigated. The $TM_{01\delta}$ and $TM_{02\delta}$ modes of the cylindrical DRA have been applied to form the wideband antenna. The DRA was simply excited by four printed arced apertures. In this way, no hole-drilling, shorting pins or meander lines are required for the fabrication. The effect of the aperture number and position on the performance of the DRA have been investigated. The results show that four apertures are enough for exciting a good omnidirectional DRA. Also, the impedance bandwidth of the DRA can be optimized by adjusting the aperture position. For demonstration, an apertures-fed low-height cylindrical DRA ($h = 0.108\ \lambda_0$) with an impedance bandwidth of ~ 34 % has been designed. The bandwidth enhancement of the proposed design is significant by compared with other low-height TM-mode DRAs. It is worth mentioning that the proposed DRA is relatively fat. This is reasonable because for a certain resonant frequency, the lower the height, the greater the radius (formula (A1)).

APPENDIX

In [2], using the "magnetic wall" method (MWM), the $TM_{0n\delta}$ -mode resonance frequency (f_0) of the cylindrical DRA can be calculated by using the formula as follows:

$$f_0 = \frac{c\sqrt{\left(X'_{0n}\right)^2 + \left(\frac{\pi a}{2h}\right)^2}}{2\pi a\sqrt{\varepsilon_r}}, J'_0\left(X'_{0n}\right) = 0 (n = 1, 2, 3 \ldots) \tag{A1}$$

where a, h, and ε_r present the radius, height, and permittivity of the cylindrical DRA, respectively, and c denotes the speed of light in vacuum. $J_0(X)$ is zero-order Bessel function of the first kind and a prime of a function denotes a derivative with respect to the argument.

REFERENCES

[1] S. Long, M. McAllister, and L. C. Shen, "The resonant cylindrical dielectric cavity antenna," *IEEE Trans. Antennas Propag.*, vol. AP-31, no. 3, pp. 406–412, May 1983.
[2] K. M. Luk and K. W. Leung, *Dielectric Resonator Antennas*. Baldock, U.K.: Research Studies Press, 2003.
[3] A. Petosa, *Dielectric Resonator Antenna Handbook*. Norwood, MA, USA: Artech House, 2007.
[4] A. Petosa and A. Ittipiboon, "Dielectric resonator antennas: A historical review and the current state of the art," *IEEE Antennas Propag. Mag.*, vol. 52, no. 5, pp. 91–116, Oct. 2010.
[5] X. S. Fang, L. P. Weng, and Y. X. Sun, "Wideband and bandwidth-controllable hybrid-cylindrical glass dielectric resonator antenna for indoor communication," *IEEE Access*, vol. 8, pp. 50414–50420, 2020.
[6] L. K. Hady, D. Kajfez, and A. A. Kishk, "Triple mode use of a single dielectric resonator," *IEEE Trans. Antennas Propag.*, vol. 57, no. 5, pp. 1328–1335, May 2009.
[7] N. Yang, K. W. Leung, K. Lu, and N. Wu, "Omnidirectional circularly polarized dielectric resonator antenna with logarithmic spiral slots in the ground," *IEEE Trans. Antennas Propag.*, vol. 65, no. 2, pp. 839–844, Feb. 2017.
[8] W. W. Li and K. W. Leung, "Omnidirectional circularly polarized dielectric resonator antenna with top-loaded Alford loop for pattern diversity design," *IEEE Trans. Antennas Propag.*, vol. 61, no. 8, pp. 4246–4256, Aug. 2013.
[9] X. S. Fang, K. W. Leung, and K. M. Luk, "Theory and experiment of three-port polarization-diversity cylindrical dielectric resonator antenna," *IEEE Trans. Antennas Propag.*, vol. 62, no. 10, pp. 4945–4951, Oct. 2014.
[10] R. K. Mongia, "Small eletric monopole mode dielectric resonator antenna," *Electron. Lett.*, vol. 32, no. 11, pp. 947–949, May 1996.
[11] R. Mongia, "Reduced size metallized dielectric resonator antennas," in *IEEE Antennas Propag. Soc. Int. Symp. Dig.*, vol. 4, Jul. 1997, pp. 2202–2205.
[12] W. Deng and S. Zheng, "A low-profile omnidirectional dielectric resonator antenna with enhanced bandwidth," in *Proc. Int. Workshop Electromagn., Appl. Student Innov. Competition (iWEM)*, Oct. 2020, pp. 1–5.
[13] L. K. Hady, A. A. Kishk, and D. Kajfez, "Dual-band compact DRA with circular and monopole-like linear polarizations as a concept for GPS and WLAN applications," *IEEE Trans. Antennas Propag.*, vol. 57, no. 9, pp. 2591–2598, Sep. 2009.
[14] S.-J. Guo, L.-S. Wu, K. W. Leung, and J.-F. Mao, "Microstrip-fed differential dielectric resonator antenna and array," *IEEE Antennas Wireless Propag. Lett.*, vol. 17, no. 9, pp. 1736–1739, Sep. 2018.
[15] A. Rashidian, M. T. Aligodarz, L. Shafai, and D. M. Klymyshyn, "On the matching of microstrip-fed dielectric resonator antennas," *IEEE Trans. Antennas Propag.*, vol. 61, no. 10, pp. 5291–5296, Oct. 2013.
[16] A. B. Kakade and B. Ghosh, "Efficient technique for the analysis of microstrip slot coupled hemispherical dielectric resonator antenna," *IEEE Antennas Wireless Propag. Lett.*, vol. 7, pp. 332–336, 2008.
[17] M. Zou, J. Pan, and Z. Nie, "A wideband circularly polarized rectangular dielectric resonator antenna excited by an Archimedean spiral slot," *IEEE Antennas Wireless Propag. Lett.*, vol. 14, pp. 446–449, 2015.

[18] Y. Gao, Z. Feng, and L. Zhang, "Compact CPW-fed dielectric resonator antenna with dual polarization," *IEEE Antennas Wireless Propag. Lett.*, vol. 10, pp. 544–547, 2011.
[19] B. Ghosh, K. Ghosh, and C. S. Panda, "Coplanar waveguide feed to the hemispherical DRA," *IEEE Trans. Antennas Propag.*, vol. 57, no. 5, pp. 1567–1571, May 2009.
[20] Z. Song, H. Zheng, M. Wang, Y. Li, T. Song, E. Li, and Y. Li, "Equilateral triangular dielectric resonator and metal patch hybrid antenna for UWB application," *IEEE Access*, vol. 7, pp. 119060–119068, 2019.
[21] M. Abedian, H. Oraizi, S. K. A. Rahim, S. Danesh, M. R. Ramli, and M. H. Jamaluddin, "Wideband rectangular dielectric resonator antenna for low-height applications," *IET Microw., Antennas Propag.*, vol. 12, no. 1, pp. 115–119, Jun. 2018.
[22] W. W. Li, K. W. Leung, and N. Yang, "Omnidirectional dielectric resonator antenna with a planar feed for circular polarization diversity design," *IEEE Trans. Antennas Propag.*, vol. 66, no. 3, pp. 1189–1197, Mar. 2018.
[23] N. Yang and K. W. Leung, "Size reduction of omnidirectional cylindrical dielectric resonator antenna using a magnetic aperture source," *IEEE Trans. Antennas Propag.*, vol. 68, no. 4, pp. 3248–3253, Apr. 2020.
[24] X. S. Fang, L. P. Weng, and Y.-X. Sun, "Slots-coupled omnidirectional circularly polarized cylindrical glass dielectric resonator antenna for 5.8-GHz WLAN application," *IEEE Access*, vol. 8, pp. 204718–204727, 2020.

XIAO SHENG FANG (Member, IEEE) received the B.Eng. degree in electronic engineering from Sun Yat-sen University, Guangzhou, China, in 2008, and the Ph.D. degree in electronic engineering from the City University of Hong Kong, Hong Kong, in 2012. From 2012 to 2015, he was a Senior Research Assistant with the Department of Electronic Engineering, City University of Hong Kong. He is currently an Associate Professor with the Department of Electronic Engineering, Shantou University, Shantou, China. His research interests include microwave antennas, dielectric resonator antennas, and passive RF components. He is currently serving as a Technical Reviewer for the IEEE TRANSACTIONS ON ANTENNAS AND PROPAGATION, the IEEE ANTENNAS AND WIRELESS PROPAGATION LETTERS, and IEEE ACCESS.

LING PENG WENG (Student Member, IEEE) was born in Fuzhou, Fujian, China, in 1995. He received the B.E. degree in electronics and information engineering from Huaqiao University, in 2017, and the master's degree in engineering from Shantou University, in 2021. He is currently an Antenna Engineer with Hytera Communications Corporation Ltd., Shenzhen, China. His research interests include dielectric resonator antennas, microwave antennas, and wireless communication.

ZHUN FAN (Senior Member, IEEE) received the B.S. and M.S. degrees in control engineering from the Huazhong University of Science and Technology, Wuhan, China, in 1995 and 2000, respectively, and the Ph.D. degree in electrical and computer engineering from Michigan State University, Lansing, MI, USA, in 2004. He was an Associate Professor with the Technical University of Denmark, from 2007 to 2011, the Department of Mechanical Engineering, and the Department of Management Engineering; and an Assistant Professor with the Department of Mechanical Engineering, Technical University of Denmark, from 2004 to 2007. He is currently a Full Professor with Shantou University (STU), Shantou, China. He serves as the Head of the Department of Electrical Engineering and the Director for the Guangdong Provincial Key Laboratory of Digital Signal and Image Processing. He has been a Principle Investigator of a number of projects from the Danish Research Agency of Science Technology and Innovation and the National Natural Science Foundation of China. His major research interests include intelligent control and robotic systems, robot vision and cognition, MEMS, computational intelligence, design automation, optimization of mechatronic systems, machine learning, and image processing.